Ultraslow optical solitons via electromagnetically induced transparency: a density-matrix approach*

Luo Bin(骆 斌)[a)b)], Hang Chao(杭 超)[b)], Li Hui-Jun(李慧军)[c)], and Huang Guo-Xiang(黄国翔)[b)c)]

[a)] *Department of Physics and Information Science, Yulin Teachers College, Yulin* 537000, *China*
[b)] *Department of Physics, East China Normal University, Shanghai* 200062, *China*
[c)] *Department of Physics, Zhejiang Normal University, Jinhua* 321004, *China*

(Received 29 October 2008; revised manuscript received 22 September 2009)

We study the ultraslow optical solitons in a resonant three-level atomic system via electromagnetically induced transparency under a density-matrix (DM) approach. The results of linear and nonlinear optical properties are compared with those obtained by using an amplitude variable (AV) approach. It is found that the results for both approaches are the same in the linear regime if the corresponding relations between the population-coherence decay rates in the DM approach and the energy-level decay rates in the AV approach are appropriately imposed. However, in the nonlinear regime there is a small difference for the self-phase modulation coefficient of the nonlinear Schrödinger equation that governs the time evolution of probe pulse envelope. All analytical predicts are checked by numerical simulations.

Keywords: ultraslow optical solitons, electromagnetically induced transparency
PACC: 4265S, 4225B

1. Introduction

Solitons, which are known as a class of shaping-preserving wave propagation phenomena in nonlinear media, have attracted much attention in recent years.[1]. These special types of wave packets appear as the result of interplay between nonlinearity and dispersion and hence can propagate undistortedly over long distance. Solitons have been discovered in many branches of physics and states of matters ranging from solid medium, such as superconducting Josephson junctions (magnetic flux solitons[1]), to Bose–Einstein condensed atomic vapour (matter wave solitons[2]).

Solitons in optical domain are of special interest because of their important applications for information processing and transmission.[3] Up to now, most optical solitons are produced in passive optical media such as glass-based optical fibres, in which far-off resonance excitation schemes are generally employed in order to avoid unmanageable optical attenuation and distortion. However, due to the lack of distinctive energy levels, the nonlinear effect in such passive optical media is very weak, and hence to form a soliton a very high light intensity is required. As a consequence, optical solitons produced in this way generally travel with a speed very close to c, the speed of light in vacuum. In addition, the lack of distinctive energy levels and transition selection rules also makes an active control of such optical soliton difficult.

In recent years, much attention has been paid to the studies on the optical property of an active optical medium via electromagnetically induced transparency (EIT),[4] in which an on-resonance excitation scheme is employed. Due to the quantum interference effect induced by a control field, the wave propagation of a weak probe field in such medium displays many striking features,[5] including a large suppression of optical absorption and a significant reduction of group velocity.[6,7] Based on these interesting features, it has been shown that a new type of optical solitons, i. e. ultraslow optical solitons, can form in resonant multi-level media.[8−16] Up to now all investigations on the ultraslow optical solitons in the EIT-based systems[8−20] are analysed by using amplitude variable (AV) approach. The advantage of such approach is its simplicity in analytical and numerical calculations. However, from physical point of view a sounder analysis should adopt density-matrix (DM) formulism.[21] This raises a question of comparing quantitatively the results obtained by using the AV and DM approaches and finding the relations and correspondences between them.

In this work, we present a study on the ultraslow

*Project supported by National Natural Science Foundation of China (Grant Nos. 10674060, 10874043 and 10974181), by the National Basic Research Program of China (Grant Nos. 2005CB724508 and 2006CB921104).
© 2010 Chinese Physical Society and IOP Publishing Ltd

optical solitons in a cold, highly resonant atomic system via EIT by employing a DM approach. A method of multiple-scales for nonlinear excitations in such resonant system described by DM equations of motion is developed. We show that in the linear regime both approaches give the same results if the corresponding relations between the population-coherence decay rates in the DM approach and the energy-level decay rates in the AV approach are suitably imposed. In the nonlinear regime, however, there is a small difference for the self-phase modulation coefficient of the nonlinear Schrödinger equation that governs the time evolution of probe pulse envelope. All analytical predicts are checked by numerical simulations and good agreement is found.

The paper is arranged as follows. In Section 2, we describe the physical model of a three-state Λ-type system under both the DM and the AV formulisms. In Section 3, we make a comparison between the linear solutions obtained from the DM and AV approaches. In Section 4, we derive a nonlinear envelope equation governing the motion of probe field envelope. In Section 5, the difference between the self-phase modulation coefficients obtained from the DM and AV approaches is illustrated. An ulatraslow optical soliton is also given under a realistic set of system parameters. The last section (Section 6) contains a discussion and summary of our main results of this work.

2. Equations of motion in the DM and the AV approaches

The physical system under study is a resonant, lifetime broadened three-state noninteracting atomic system with a Λ configuration, shown in Fig. 1. Atoms of the system interact with a strong, continuous-wave control field of angular frequencies $\omega_{\rm c}$ ($|2\rangle \leftrightarrow |3\rangle$) and a weak, pulsed probe field (with the pulse length τ_0 at the entrance of the medium) of centre angular frequency $\omega_{\rm p}$ ($|1\rangle \leftrightarrow |3\rangle$). The electric-field vector of the system can be written as $\boldsymbol{E} = \sum_{l={\rm p,c}} \boldsymbol{e}_l \mathcal{E}_l \exp[{\rm i}(\omega_l/c)(z-ct)] + {\rm c.c.}$, where $\boldsymbol{e}_{\rm p}$ ($\boldsymbol{e}_{\rm c}$) is the unit vector denoting the polarization of the probe (coupling) laser field with the envelope $\mathcal{E}_{\rm p}$ ($\mathcal{E}_{\rm c}$). The state vector of the system is $|\Psi\rangle = \sum_{j=1}^{3} A_j \exp[{\rm i}(k_j z - (E_j/\hbar + \Delta_j)t]|j\rangle$. Here $\Delta_1 = 0$, $\Delta_2 = \omega_{\rm p} - \omega_{\rm c} - (E_2 - E_1)/\hbar$ (two-photon detuning), $\Delta_3 = \omega_{\rm p} - (E_3 - E_1)/\hbar$ (one-photon detuning), $k_1 = 0$, $k_2 = k_{\rm p} - k_{\rm c}$, $k_3 = k_{\rm p}$, and $|j\rangle$ are the bare-state base vectors of an atom with eigenenergy E_j ($j = 1$–3). Under electric-dipole and rotating-wave approximations, the Hamiltonian of the system in the Schrödinger picture reads

$$H = \sum_{j=1}^{3} E_j|j\rangle\langle j| - \hbar[\Omega_{\rm p}^* {\rm e}^{{\rm i}(k_{\rm p}z-\omega_{\rm p}t)}|1\rangle\langle 3| + \Omega_{\rm c}^* {\rm e}^{{\rm i}(k_{\rm c}z-\omega_{\rm c}t)}|2\rangle\langle 3| + {\rm h.c.}], \quad (1)$$

where $\Omega_{\rm p} = \boldsymbol{e}_{\rm p} \cdot \boldsymbol{p}_{31}\mathcal{E}_{\rm p}/\hbar$ ($\Omega_{\rm c} = \boldsymbol{e}_{\rm c} \cdot \boldsymbol{p}_{32}\mathcal{E}_{\rm c}/\hbar$) is the half Rabi frequency corresponding to the probe (controlling) optical field, with $\boldsymbol{p}_{ij}$ being the electric dipole matrix element associated with the transition from $|j\rangle$ to $|i\rangle$.

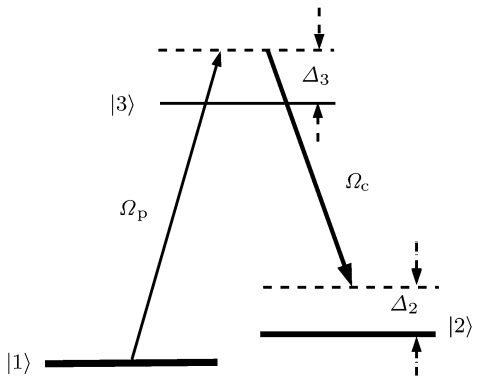


Fig. 1. The energy levels $|j\rangle$ ($j = 1, 2, 3$) and excitation scheme of a lifetime broadened three-state atomic system interacting with a strong, continuous wave control field of Rabi frequencies $\Omega_{\rm c}$ and a weak, pulsed probe field of Rabi frequency $\Omega_{\rm p}$. Δ_2 and Δ_3 are one-photon and two-photon detunings, respectively.

In order to investigate the time evolution of the system, it is more convenient to employ an interaction picture. The Hamiltonian in the interaction picture is

$$H_{\rm int} = -\hbar[\Delta_2|2\rangle\langle 2| + \Delta_3|3\rangle\langle 3| + \Omega_{\rm p}^*|1\rangle\langle 3| + \Omega_{\rm c}^*|2\rangle\langle 3| + {\rm h.c.}].$$

In the DM approach,[21] the evolution of density matrix $\sigma_{ij} \equiv A_i A_j^*$ is controlled by the equations

$${\rm i}\frac{\partial}{\partial t}\sigma_{11} - {\rm i}\,\Gamma_{31}\sigma_{33} + \Omega_{\rm p}^*\sigma_{31} - \Omega_{\rm p}\sigma_{31}^* = 0, \quad (2a)$$

$${\rm i}\frac{\partial}{\partial t}\sigma_{22} - {\rm i}\,\Gamma_{32}\sigma_{33} + \Omega_{\rm c}^*\sigma_{32} - \Omega_{\rm c}\sigma_{32}^* = 0, \quad (2b)$$

$${\rm i}\left(\frac{\partial}{\partial t} + \Gamma_3\right)\sigma_{33} - \Omega_{\rm p}^*\sigma_{31} + \Omega_{\rm p}\sigma_{31}^* - \Omega_{\rm c}^*\sigma_{32} + \Omega_{\rm c}\sigma_{32}^* = 0, \quad (2c)$$

for diagonal elements, and

$$\left({\rm i}\frac{\partial}{\partial t} + d_{21}\right)\sigma_{21} - \Omega_{\rm p}\sigma_{32}^* + \Omega_{\rm c}^*\sigma_{31} = 0, \quad (3a)$$

$$\left({\rm i}\frac{\partial}{\partial t} + d_{31}\right)\sigma_{31} - \Omega_{\rm p}(\sigma_{33} - \sigma_{11}) + \Omega_{\rm c}\sigma_{21} = 0, \quad (3b)$$

$$\left(\mathrm{i}\frac{\partial}{\partial t}+d_{32}\right)\sigma_{32}-\Omega_{\mathrm{c}}(\sigma_{33}-\sigma_{22})+\Omega_{\mathrm{p}}\sigma_{21}^{*}=0, \quad (3c)$$

for non-diagonal elements, where $d_{ij}=\Delta_i-\Delta_j+\mathrm{i}\,\gamma_{ij}$ $(i,j=1,2,3)$. The population and coherence decay rates are defined by $\Gamma_i=\sum_{E_j<E_i}\Gamma_{ij}$ and $\gamma_{ij}=\frac{1}{2}(\Gamma_i+\Gamma_j)+\frac{1}{2}(\gamma_i+\gamma_j)+\gamma_{ij}^{\mathrm{col}}$, respectively. Here Γ_{ij} is the spontaneous emission decay rate from $|i\rangle$ to $|j\rangle$, γ_i is the ionization rate of state $|j\rangle$, and $\gamma_{ij}^{\mathrm{col}}$ denotes the dipole dephasing rate caused by collisions. For simplicity, we have assumed that the transition between states $|1\rangle$ and $|2\rangle$ is forbidden and hence $\Gamma_{21}=0$. From the first three equations we have obviously $\sum_{j=1}^{3}\sigma_{jj}=1$, which means that no atom can escape from the system. Thus, we may use the relation $\sigma_{33}=1-\sigma_{11}-\sigma_{22}$ to replace Eq. (2c).

The equation of motion for $\Omega_{\mathrm{p}}(x,y,z,t)$ can be obtained by the Maxwell equation $\nabla^2\boldsymbol{E}-(1/c^2)\partial^2\boldsymbol{E}/\partial t^2=[1/(\varepsilon_0c^2)]\partial^2\boldsymbol{P}/\partial t^2$, with

$$\begin{aligned}\boldsymbol{P}=\mathcal{N}_a[&\boldsymbol{p}_{13}\sigma_{31}\exp[\mathrm{i}(k_{\mathrm{p}}z-\omega_{\mathrm{p}}t)]\\&+\boldsymbol{p}_{23}\sigma_{32}\exp[\mathrm{i}(k_{\mathrm{c}}z-\omega_{\mathrm{c}}t)]+\mathrm{c.c.}],\end{aligned}$$

where $\mathcal{N}_a$ is atomic concentration. Under slowly-varying envelope approximation, the Maxwell equation reduces to

$$\mathrm{i}\left(\frac{\partial}{\partial z}+\frac{1}{c}\frac{\partial}{\partial t}\right)\Omega_{\mathrm{p}}+\frac{c}{2\omega_{\mathrm{p}}}\left(\frac{\partial^2}{\partial x^2}+\frac{\partial^2}{\partial y^2}\right)\Omega_{\mathrm{p}}+\kappa\sigma_{31}=0, \quad (4)$$

where $\kappa=\mathcal{N}_a\omega_{\mathrm{p}}|\boldsymbol{p}_{13}|^2/(2\epsilon_0c\hbar)$. Equations (3) and (4) are the basic controlling equations in the MD approach (called the Maxwell–Bloch equations).[21]

The system can also be described in another way, i. e. by the Maxwell–Schrödinger equations

$$\left(\mathrm{i}\frac{\partial}{\partial t}+d_2\right)A_2+\Omega_{\mathrm{c}}^{*}A_3=0, \quad (5a)$$

$$\left(\mathrm{i}\frac{\partial}{\partial t}+d_3\right)A_3+\Omega_{\mathrm{p}}A_1+\Omega_{\mathrm{c}}A_2=0, \quad (5b)$$

$$|A_1|^2+|A_2|^2+|A_3|^2=1, \quad (5c)$$

$$\mathrm{i}\left(\frac{\partial}{\partial z}+\frac{1}{c}\frac{\partial}{\partial t}\right)\Omega_{\mathrm{p}}+\frac{c}{2\omega_{\mathrm{p}}}\left(\frac{\partial^2}{\partial x^2}+\frac{\partial^2}{\partial y^2}\right)\Omega_{\mathrm{p}}+\kappa A_3A_1^{*}=0, \quad (5d)$$

where $d_j=\Delta_j+\mathrm{i}\,\gamma_j^{\mathrm{AV}}$ with γ_j^{AV} describing the decay rate of the energy level $|j\rangle$. Equations (5) are the basic equations employed in the AV approach, which have been used in Refs. [9] and [10] for the study of the ultraslow optical solitons in the same system.

3. Solutions in linear regime

We first find the linear solution in the MD approach and make a comparison with that obtained in the AV approach. We assume that the atoms are initially populated in the state $|1\rangle$. In the linear regime the probe field is very weak and the ground state is not depleted during evolution, i. e. $\sigma_{11}\approx1$ and $\sigma_{jj}\approx\sigma_{32}\approx0$ $(j=2,3)$. In this situation the Maxwell–Bloch Eqs. (3) and (4) are linearized and the solution can be easily obtained as

$$\Omega_{\mathrm{p}}=F\exp\{\mathrm{i}[K(\omega)z-\omega t]\}, \quad (6a)$$

$$\sigma_{j1}=\frac{\delta_{j3}(\omega+d_{21})-\delta_{j2}\Omega_{\mathrm{c}}^{*}}{D(\omega)}F\exp\{\mathrm{i}[K(\omega)z-\omega t]\}, \quad (j=2,3), \quad (6b)$$

where F is a constant. $K(\omega)$ is the linear dispersion relation of the system

$$K(\omega)=\frac{\omega}{c}+\frac{\kappa(\omega+d_{21})}{D(\omega)}, \quad (7)$$

with $D(\omega)=|\Omega_{\mathrm{c}}|^2-(\omega+d_{21})(\omega+d_{31})$. In obtaining Eq. (7) we have neglected the transverse diffraction effect which is usually very small for the leading order of Eq. (4). In most operation conditions $K(\omega)$ can be Taylor expanded around the centre frequency ω_{p} of the probe field, that is, $\omega=0$. We thus have

$$K(\omega)=K_0+K_1\omega+\frac{1}{2}K_2\omega^2+\ldots, \quad (8)$$

where $K_j=[\partial^jK(\omega)/\partial\omega^j]|_{\omega=0}$ $(j=0,1,2,\ldots)$. These dispersion coefficients can be obtained analytically. Here, $K_0=\phi+\mathrm{i}\,\alpha/2$ gives the phase shift ϕ per unit length and absorption coefficient α of the probe field, $1/K_1$ is related to the group velocity, and K_2 describes the group velocity dispersion (i.e., pulse spreading). For probe field with a Gaussian input form, i.e., $\Omega_{\mathrm{p}}(0,t)=\Omega_{\mathrm{p}}(0,0)\exp(-t^2/\tau_0^2)$, we have[10]

$$\Omega_{\mathrm{p}}(z,t)=\frac{\Omega_{\mathrm{p}}(0,0)}{\sqrt{b_1(z)-\mathrm{i}\,b_2(z)}}\times\exp\left[\mathrm{i}\,K_0z-\frac{(K_1z-t)^2}{[b_1(z)-\mathrm{i}\,b_2(z)]\tau_0^2}\right],$$

where $b_1(z)=1+2z\mathrm{Im}(K_2)/\tau_0^2$ and $b_2(z)=2z\mathrm{Re}(K_2)/\tau_0^2$. The above equation clearly shows the dispersion (i.e. non-adiabatic) effects contributed by K_1 and K_2.

In the same way, we can obtain the linear solution of the system under the AV approach (i.e. by solving the Eqs. (5a)–(5d) with $A_1\approx1$), which reads[10]

$$A_j = \frac{-\delta_{j2}\Omega_{\rm c}^* + \delta_{j3}(\omega + d_2)}{D(\omega)} F \exp\{{\rm i}[K^{\rm AV}(\omega)z - \omega t]\}, \quad (j = 2, 3). \tag{9}$$

The half Rabi frequency of the probe field is the same as that given by Eq. (6a). The linear dispersion function obtained by the AV approach reads

$$K^{\rm AV}(\omega) = \frac{\omega}{c} + \frac{\kappa(\omega + d_2)}{D^{\rm AV}(\omega)}, \tag{10}$$

where $D^{\rm AV}(\omega) = |\Omega_{\rm c}|^2 - (\omega + d_2)(\omega + d_3)$. By Taylor expanding Eq. (10) around the centre frequency of the probe field one can also obtain the expansion coefficients K_0, K_1 and K_2. The linear dispersion coefficients obtained from the DM and the AV approaches, respectively are listed in Table 1.

Table 1. Dispersion coefficients obtained from the density matrix approach (DMA) and the amplitude variable approach (AVA).

	K_0	K_1	K_2
DMA	$\frac{\kappa d_{21}}{\lvert\Omega_{\rm c}\rvert^2 - d_{21}d_{31}}$	$\frac{1}{c} + \frac{\kappa(\lvert\Omega_{\rm c}\rvert^2 + d_{21}^2)}{(\lvert\Omega_{\rm c}\rvert^2 - d_{21}d_{31})^2}$	$2\frac{\kappa(d_{31}\lvert\Omega_{\rm c}\rvert^2 + 2d_{21}\lvert\Omega_{\rm c}\rvert^2 + d_{21}^3)}{(\lvert\Omega_{\rm c}\rvert^2 - d_{21}d_{31})^3}$
AVA	$\frac{\kappa d_2}{\lvert\Omega_{\rm c}\rvert^2 - d_2 d_3}$	$\frac{1}{c} + \frac{\kappa(\lvert\Omega_{\rm c}\rvert^2 + d_2^2)}{(\lvert\Omega_{\rm c}\rvert^2 - d_2 d_3)^2}$	$2\frac{\kappa(d_3\lvert\Omega_{\rm c}\rvert^2 + 2d_2\lvert\Omega_{\rm c}\rvert^2 + d_2^3)}{(\lvert\Omega_{\rm c}\rvert^2 - d_2 d_3)^3}$

Obviously, if the following corresponding relations

$$\gamma_2^{\rm AV} \leftrightarrow \gamma_{21} = \frac{1}{2}(\gamma_2 + \gamma_1) + \gamma_{21}^{\rm col}, \tag{11a}$$

$$\gamma_3^{\rm AV} \leftrightarrow \gamma_{31} = \frac{1}{2}(\Gamma_{31} + \Gamma_{32}) + \frac{1}{2}(\gamma_3 + \gamma_1) + \gamma_{31}^{\rm col}, \tag{11b}$$

are imposed, we obtain $K(\omega) = K^{\rm AV}(\omega)$ and hence $K_j(\omega) = K_j^{\rm AV}(\omega)$ ($j = 0$ to 2). In this way, the AV approach and the DM approach give the same linear solution of the system.

The linear susceptibilities of the probe field under the DM and the AV approaches are defined by $\chi(\omega) = \mathcal{N}_a|\boldsymbol{p}_{13}|^2\sigma_{31}/(\epsilon_0\hbar\Omega_{\rm p})$ and $\chi^{\rm AV}(\omega) = \mathcal{N}_a|\boldsymbol{p}_{13}|^2 A_3 A_1^*/(\epsilon_0\hbar\Omega_{\rm p})$, respectively, i.e.

$$\chi(\omega) = \frac{\mathcal{N}_a|\boldsymbol{p}_{13}|^2}{\epsilon_0\hbar}\frac{\omega + d_{21}}{D(\omega)}, \tag{12a}$$

$$\chi^{\rm AV}(\omega) = \frac{\mathcal{N}_a|\boldsymbol{p}_{13}|^2}{\epsilon_0\hbar}\frac{\omega + d_2}{D^{\rm AV}(\omega)}. \tag{12b}$$

Under the correspondence relation (11), we have $\chi(\omega) = \chi^{\rm AV}(\omega)$. In Fig. 2 we plot the curves of the dispersion and absorption spectra which are determined by Re$[\chi(\omega)]$ (solid line) and Im$[\chi(\omega)]$ (dashed line), respectively. The parameters are taken as $\gamma_{21} = 1$ kHz, $\gamma_{31} = 5$ MHz, $\kappa = 1.0 \times 10^9$ cm$^{-1}\cdot$s^{-1}, $\Omega_{\rm c} = 1.6 \times 10^7$ s^{-1}, and $\Delta_2 = \Delta_3 = 0$. We see that near the central frequency of the probe field ($\omega = 0$) one has Im$[\chi(\omega)] \approx 0$, i.e. the absorption of the probe field is largely suppressed. As a result, a transparency window opens for the probe field due to the introduction of the control field. The positive slope of the curve of Re$[\chi(\omega)]$ (i.e. normal dispersion) near $\omega = 0$ corresponds to an ultraslow propagation of the probe field as we shall see below.

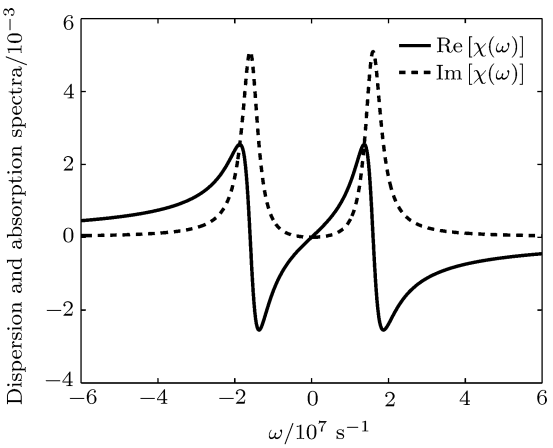


Fig. 2. The curves of Re$[\chi(\omega)]$ (solid line) and Im$[\chi(\omega)]$ (dashed line) versus ω. The parameters are given in the text. Due to the contribution of the control field a transparency window open for the probe field propagation.

4. Asymptotic expansion and envelope equation

We now turn to investigate the nonlinear evolution of the probe pulse by solving the DM equations of motion (3) and (4). To obtain a shape-preserving nonlinear pulse, two-photon detuning Δ_2 must be nonvanishing, which provides not only ultraslow propagation but also necessary nonlinearity that can balance the dispersion effect. We extend the method of multiple-

scales widely used in the AV approach[8−18,20] into the present DM approach to derive the nonlinear envelope equation of the probe field envelope. We take the following asymptotic expansion

$$\sigma_{11} = 1 + \epsilon^2\sigma_{11}^{(2)} + \epsilon^3\sigma_{11}^{(3)} + \ldots, \tag{13a}$$

$$\sigma_{22} = \epsilon^2\sigma_{22}^{(2)} + \epsilon^3\sigma_{22}^{(3)} + \ldots, \tag{13b}$$

$$\sigma_{j1} = \epsilon\sigma_{j1}^{(1)} + \epsilon^2\sigma_{j1}^{(2)} + \epsilon^3\sigma_{21}^{(3)} + \ldots, \quad (j = 2, 3), \tag{13c}$$

$$\sigma_{32} = \epsilon^2\sigma_{32}^{(2)} + \epsilon^3\sigma_{32}^{(3)} + \ldots, \tag{13d}$$

$$\Omega_{\rm p} = \epsilon\Omega_{\rm p}^{(1)} + \epsilon^2\Omega_{\rm p}^{(2)} + \epsilon^3\Omega_{\rm p}^{(3)} + \ldots, \tag{13e}$$

where ϵ is a dimensionless small parameter characterizing the amplitude of the probe field. To obtain a divergence-free expansion, all quantities on the right hand side of the expansion are considered as functions of the multi-scale variables $z_l = \epsilon^l z$ ($l = 0$ to 2), $t_l = \epsilon^l t$ ($l = 0$, 1), $x_1 = \epsilon x$, and $y_1 = \epsilon y$. Substituting expansion (13) into equations (3) and (4), we obtain a chain of linear, but inhomogeneous equations

$$\mathrm{i}\left(\frac{\partial}{\partial z_0} + \frac{1}{c}\frac{\partial}{\partial t_0}\right)\Omega_{\rm p}^{(l)} + \kappa\sigma_{31}^{(l)} = M^{(l)}, \tag{14a}$$

$$\left(\mathrm{i}\frac{\partial}{\partial t_0} + d_{21}\right)\sigma_{21}^{(l)} + \Omega_{\rm c}^*\sigma_{31}^{(l)} = N^{(l)}, \tag{14b}$$

$$\left(\mathrm{i}\frac{\partial}{\partial t_0} + d_{31}\right)\sigma_{31}^{(l)} + \Omega_{\rm p}^{(l)} + \Omega_{\rm c}\sigma_{21}^{(l)} = P^{(l)}, \tag{14c}$$

$$\left(\mathrm{i}\frac{\partial}{\partial t_0} + d_{32}\right)\sigma_{32}^{(l)} + \Omega_{\rm c}(\sigma_{11}^{(l)} + 2\sigma_{22}^{(l)}) = Q^{(l)}, \tag{14d}$$

$$\mathrm{i}\frac{\partial}{\partial t_0}\sigma_{11}^{(l)} + \mathrm{i}\,\Gamma_{13}(\sigma_{11}^{(l)} + \sigma_{22}^{(l)}) = Y^{(l)}, \tag{14e}$$

$$\mathrm{i}\frac{\partial}{\partial t_0}\sigma_{22}^{(l)} + \mathrm{i}\,\Gamma_{23}(\sigma_{11}^{(l)} + \sigma_{22}^{(l)}) + \Omega_{\rm c}^*\sigma_{32}^{(l)} - \Omega_{\rm c}\sigma_{32}^{*(l)} = Z^{(l)}. \tag{14f}$$

The explicit expressions of $M^{(l)}$, $N^{(l)}$, $P^{(l)}$, $Q^{(l)}$, $Y^{(l)}$ and $Z^{(l)}$ can be systematically obtained but omitted here for saving space.

At the leading order (i.e. $l = 1$), Eqs. (14a)–(14f) give the solution in the linear regime, which reads

$$\Omega_{\rm p}^{(1)} = F\,\exp(\mathrm{i}\,\theta), \tag{15a}$$

$$\sigma_{j1}^{(1)} = \frac{\delta_{j3}(\omega + d_{21}) - \delta_{j2}\Omega_{\rm c}^*}{D(\omega)}F\mathrm{e}^{\mathrm{i}\,\theta}, \quad (j = 2, 3) \tag{15b}$$

with $\theta = K(\omega)z_0 - \omega t_0$. Obviously, the above solution coincides with the result given in Eq. (6) if F is taken being a constant. Here we assume F being a yet to be determined envelope function depending on the slow variables x_1, y_1, t_1 and z_j ($j = 1$, 2). One of the aims for doing this is to eliminate the divergence that will appear in the high-order solutions.

To the next order ($l = 2$), a divergence-free condition for the second-order solution requires $\mathrm{i}[\partial F/\partial z_1 + (1/V_{\rm g})\partial F/\partial t_1] = 0$, where $V_{\rm g} = 1/K_1$ is the group velocity of the envelope F. Under such condition we have

$$\sigma_{31}^{(2)} = \frac{\mathrm{i}}{\kappa}\left(\frac{1}{V_{\rm g}} - \frac{1}{c}\right)\frac{\partial F}{\partial t_1}\mathrm{e}^{\mathrm{i}\,\theta}, \tag{16a}$$

$$\sigma_{21}^{(2)} = -\frac{\mathrm{i}}{\Omega_{\rm c}\kappa}\left[\left(K - \frac{\omega}{c}\right) + (\omega + d_{31})\left(\frac{1}{V_{\rm g}} - \frac{1}{c}\right)\right]\frac{\partial F}{\partial t_1}\mathrm{e}^{\mathrm{i}\,\theta}, \tag{16b}$$

$$\sigma_{jj}^{(2)} = a_{jj}^{(2)}|F|^2\mathrm{e}^{-\bar{\alpha}z_2}, \quad (j = 1, 2), \tag{16c}$$

$$\sigma_{32}^{(2)} = a_{32}^{(2)}|F|^2\mathrm{e}^{-\bar{\alpha}z_2}, \tag{16d}$$

where

$$a_{11}^{(2)} = \frac{\left[\mathrm{i}\,\Gamma_{23} - 2|\Omega_{\rm c}|^2\left(\dfrac{1}{d_{32}} - \dfrac{1}{d_{32}^*}\right)\right]\left(\dfrac{\omega + d_{21}^*}{D^*} - \dfrac{\omega + d_{21}}{D}\right) - \mathrm{i}\,\Gamma_{13}|\Omega_{\rm c}|^2\left(\dfrac{1}{Dd_{32}^*} - \dfrac{1}{D^*d_{32}}\right)}{\mathrm{i}\,\Gamma_{13}|\Omega_{\rm c}|^2\left(\dfrac{1}{d_{32}^*} - \dfrac{1}{d_{32}}\right)}, \tag{17a}$$

$$a_{22}^{(2)} = \frac{1}{\mathrm{i}\,\Gamma_{13}}\left(\frac{\omega + d_{21}^*}{D^*} - \frac{\omega + d_{21}}{D} - \mathrm{i}\,\Gamma_{13}a_{11}^{(2)}\right), \tag{17b}$$

$$a_{32}^{(2)} = \frac{1}{d_{32}}\left[\frac{\Omega_{\rm c}}{D^*} - \Omega_{\rm c}(a_{11}^{(2)} + 2a_{22}^{(2)})\right], \tag{17c}$$

and $\alpha = \epsilon^2\bar{\alpha} = \mathrm{Im}[K(\omega)]$.

With the above results we go to the third order ($l = 3$). The divergence-free condition in this order yields the nonlinear Schrödinger (NLS) equation for the envelope function F:

$$\mathrm{i}\frac{\partial F}{\partial z_2} + \frac{c}{2\omega_{\rm p}}\left(\frac{\partial^2}{\partial x_1^2} + \frac{\partial^2}{\partial y_1^2}\right)F - \frac{1}{2}K_2\frac{\partial^2 F}{\partial t_1^2} - W|F|^2F\mathrm{e}^{-\bar{\alpha}z_2} = 0 \tag{18}$$

with

$$W = -\frac{\kappa}{D}[\Omega_{\rm c} a_{32}^{*(2)} + (\omega + d_{21})(2a_{11}^{(2)} + a_{22}^{(2)})],$$

characterizing the self-phase modulation (SPM) effect of the system. Under the condition $\Gamma_{21} = 0$ and $\Gamma_{31} \approx \Gamma_{32} = \Gamma$, we have $d_{21} \approx \Delta_2$, $d_{31} \approx \Delta_3 + {\rm i}\,\Gamma$ and $d_{32} \approx \Delta_3 - \Delta_2 + {\rm i}\,\Gamma$, and hence

$$W = \frac{\kappa\Delta_2}{\tilde{D}} \frac{2|\Omega_{\rm c}|^4 + \Delta_2^2[(\Delta_3 - \Delta_2)^2 + \Gamma^2] + \Delta_2(4\Delta_2 + \Delta_3 + {\rm i}\,\Gamma)|\Omega_{\rm c}|^2}{|\tilde{D}|^2|\Omega_{\rm c}|^2}, \tag{19}$$

where $\tilde{D} = |\Omega_{\rm c}|^2 - \Delta_2\Delta_3 - {\rm i}\,\Delta_2\Gamma$.

Combining the envelope equations of the second and the third order, we obtain

$${\rm i}\left(\frac{\partial}{\partial z} + \frac{\alpha}{2}\right)U + \frac{c}{2\omega_{\rm p}}\left(\frac{\partial^2}{\partial x^2} + \frac{\partial^2}{\partial y^2}\right)U - \frac{1}{2}K_2\frac{\partial^2 U}{\partial\tau^2} - W|U|^2U = 0, \tag{20}$$

after returning to original variables, where we have set $\tau = t - z/V_{\rm g}$,$U = \epsilon F{\rm e}^{-{\rm i}\,\alpha z/2}$ and $\omega = 0$.

For completeness and also for the comparison used in the following, we give a simple description on the derivation of the envelope equation for F by using the AV approach, which was given firstly in Ref. [10]. The corresponding asymptotic expansion in the AV approach is $A_j = \sum_{n=0}^{\infty}\epsilon^n A_j^{(n)} (j = 1, 2, 3)$ ($A_1^{(0)} = 1$, $A_1^{(1)} = A_2^{(0)} = A_3^{(0)} = 0$) and $\Omega_{\rm p} = \sum_{n=1}^{\infty}\epsilon^n\Omega_{\rm p}^{(n)}$. To obtain a divergence-free expansion, all quantities on the right hand side of asymptotic expansion are considered also as functions of the multi-scale variables $z_l = \epsilon^l z$ ($l = 0$ to 2), $t_l = \epsilon^l t$ ($l = 0$, 1), $x_1 = \epsilon x$ and $y_1 = \epsilon y$. Substituting the expansions and the multi-scale variables into Eq. (5), we obtain a chain of linear, but inhomogeneous equations on $A_j^{(n)}$ and $\Omega_{\rm p}^{(n)}$, which can be solved order by order.

At the leading order, $O(\epsilon)$, the solution of equations (5) is just that obtained in the linear regime. To the second order, $O(\epsilon^2)$, a divergence-free solution requires ${\rm i}[\partial F/\partial z_1 + (1/V_{\rm g}^{\rm AV})\partial F/\partial t_1] = 0$, where $V_{\rm g}^{\rm AV} = 1/K_1^{\rm AV}$ is the group velocity of the probe envelope F. To the third order, $O(\epsilon^3)$, a divergence-free condition yields the equation

$${\rm i}\,\frac{\partial F}{\partial z_2} + \frac{c}{2\omega_{\rm p}}\left(\frac{\partial^2}{\partial x_1^2} + \frac{\partial^2}{\partial y_1^2}\right)F - \frac{1}{2}K_2^{\rm AV}\frac{\partial^2 F}{\partial t_1^2} - W^{\rm AV}|F|^2F{\rm e}^{-\bar{\alpha}z_2} = 0 \tag{21}$$

with

$$W^{\rm AV} = \frac{\kappa\Delta_2(|\Omega_{\rm c}|^2 + |\Delta_2|^2)}{\tilde{D}|\tilde{D}|^2}, \tag{22}$$

where we have taken $\gamma_2^{\rm AV} \approx 0$ and $\gamma_3^{\rm AV} = \Gamma$ based on the corresponding relations (11).

Equation (23) is also a NLS equation, but its dispersion coefficient (i. e. $K_2^{\rm AV}$) and the SPM coefficient (i.e. $W^{\rm AV}$) are different from those in Eq. (20). Although under the corresponding relation (11) one has $K_2 = K_2^{\rm AV}$, the SPM coefficient W is different from $W^{\rm AV}$ even under the corresponding relation (11). However, W and $W^{\rm AV}$ have the same magnitude of order. In fact only a very small difference exists between them, as we will shown below.

5. Ultraslow optical soliton solutions

The coefficients of Eq. (20) are complex and hence it is generally not integrable. That means a soliton solution, even exists, may be highly unstable. However, due to EIT effect a practical set of system parameters can be found near the EIT transparency window so that the imaginary part of these coefficients can be made much smaller than their corresponding real part, and hence it is possible to obtain a shape-preserving, localized solution that can propagate for a rather long distance without significant distortion.

Near the EIT transparency window, Eq. (20) can be converted into the dimensionless form

$${\rm i}\,\frac{\partial u}{\partial s} + \frac{\partial^2 u}{\partial\sigma^2} + 2u|u|^2 = {\rm i}\,d_0 u + d_1\left(\frac{\partial^2}{\partial\xi^2} + \frac{\partial^2}{\partial\eta^2}\right)u, \tag{23}$$

where $s = -z/(2L_D)$, $\sigma = \tau/\tau_0$, $(\xi, \eta) = (x, y)/R_\perp$, and $u = U/U_0$. $L_D = \tau_0^2/\tilde{K}_2$ is characteristic dispersion length, $R_\perp$ is beam radius, and $U_0 = (1/\tau_0)\sqrt{\tilde{K}_2/\tilde{W}}$ is typical Rabi frequency of the signal field with tide denoting the corresponding real part of each coefficient. The dimensionless coefficients $d_0 = L_D/L_A$, $d_1 = L_D/L_{\rm diff}$ with $L_A = 1/\alpha$ being

characteristic absorption length and $L_{\rm diff} = \omega_{\rm p} R_\perp^2/c$ being characteristic diffraction length.

If $L_D \ll L_{\rm A}$ and $L_D \ll L_{\rm diff}$, i.e. $d_0 \ll 1$ and $d_1 \ll 1$, Eq. (23) reduces to the standard NLS equation $\mathrm{i}\,\partial u/\partial s + \partial^2 u/\partial\sigma^2 + 2u|u|^2 = 0$, which is completely integrable and allows multi-soliton solutions. The single bright soliton solution reads $u = 2\beta\mathrm{sech}[2\beta(\sigma-\sigma_0+4\delta s)]\exp[-2\,\mathrm{i}\,\delta\sigma - 4\,\mathrm{i}(\delta^2-\beta^2)s - \mathrm{i}\,\phi_0]$ where β, δ, σ_0, and ϕ_0 are real free parameters which determine the amplitude (as well as width), propagating velocity, initial position, and initial phase of the soliton, respectively. When taking $\beta = 1/2$ and $\delta = \sigma_0 = \phi_0 = 0$, we have $u = \mathrm{sech}\sigma\exp(\mathrm{i}\,s)$, or in terms of field

$$\Omega_{\rm p} = U\mathrm{e}^{\mathrm{i}\,\tilde{K}_0 z} = \frac{1}{\tau_0}\sqrt{\frac{\tilde{K}_2}{\tilde{W}}}\,\mathrm{sech}\left[\frac{1}{\tau_0}\left(t - \frac{z}{\tilde{V}_{\rm g}}\right)\right] \times \exp\left[\mathrm{i}\,\tilde{K}_0 z - \mathrm{i}\,\frac{z}{2L_D}\right], \qquad (24)$$

which describes a bright fundamental soliton travelling with propagating velocity $\tilde{V}_{\rm g}$.

Now we consider an atomic system which can be realized by a typical alkali atomic vapour at ultracold temperature. The parameters suitable to this system are given as $\Gamma_{31} \approx \Gamma_{32} = 2.5$ MHz with ionization rates and dipole dephasing rates being much smaller. We take $\kappa = 1.0\times10^9$ cm$^{-1}\cdot$s^{-1}, $\Omega_{\rm c} = 1.6\times10^7$ s^{-1}, $\Delta_2 = 8.0\times10^5$ s^{-1}, $\Delta_3 = 4.0\times10^7$ s^{-1}, $\lambda_{\rm p} = c/\nu_{\rm p} = 0.8\times10^{-4}$ cm, $\tau_0 = 1.0\times10^{-6}$ s and $R_\perp = 0.05$ cm. With these parameters we get $K_0 = (3.57+\mathrm{i}\,0.03)\times10^{-1}$ cm^{-1}, $K_1 = (5.11+\mathrm{i}\,0.09)\times10^{-6}$ cm$^{-1}\cdot$s, $K_2 = (1.89+\mathrm{i}\,0.16)\times10^{-12}$ cm$^{-1}\cdot$s^2, and $W = (4.16+\mathrm{i}\,0.08)\times10^{-14}$ cm$^{-1}\cdot$s^2. We see that the imaginary part of the coefficients are indeed much smaller than their corresponding real part. The physical reason for such small imaginary part is the introduction of the control field into the system, which induces a quantum destructive interference effect that suppresses largely the absorption of the probe field. When taking $\tau_0 = 1$ μs, we have the characteristic lengths $L_D = 0.5$ cm, $L_A = 31.4$ cm and $L_{\rm diff} = 196$ cm. The typical Rabi frequency is $U_0 = 6.7\times10^6$ s^{-1}. The absorption and diffraction of the probe pulse can be neglected when the propagation distance is not much longer than a dispersion length. The group velocity $\tilde{V}_{\rm g} = 6.5\times10^{-6}c$ and hence the soliton travels with an ultraslow propagating velocity.

We now estimate the input power for generating the ultraslow optical soliton by calculating Poynting's vector. The average flux of energy over carrier-wave period is

$$\bar{P} = \bar{P}_{\max}\,\mathrm{sech}^2\left[(t - z/\tilde{V}_{\rm g})/\tau_0\right]$$

with the peak power $\bar{P}_{\max} = 2\varepsilon_0 c n_{\rm p} S_0 |\mathcal{E}_{\rm p}|^2_{\max} = 2\varepsilon_0 c n_{\rm p} S_0 (\hbar/D_0)^2 \tilde{K}_2/(\tilde{W}\tau_0^2)$. Here, $n_{\rm p} = 1 + cK/\omega_{\rm p}$ is the refractive index and S_0 is the cross-section area of the probe field. Using the above parameters, we obtain $\bar{P}_{\max} = 1.5\times10^{-3}$ mW. Thus for producing such soliton, very low input light intensity is needed. This is a drastic contrast to conventional media such as optical fibres, where ps or fs laser pulses are usually needed to reach a very high peak power to bring out the enough nonlinear effect required for soliton formation.

Taking $\gamma_2^{\rm AV} \approx 0$ and $\gamma_3^{\rm AV} = 2.5$ MHz, we obtain $\tilde{V}_{\rm g}^{\rm AV} = \tilde{V}_{\rm g}$. However, in this case $W^{\rm AV} = (1.83+\mathrm{i}\,0.01)\times10^{-14}$ cm$^{-1}\cdot$s^2, $U_0^{\rm AV} = 1.0\times10^7$ s^{-1}, and $\bar{P}_{\max}^{\rm AV} = 3.4\times10^{-3}$ mW. Hence, the SPM coefficient (the peak power) obtained from the AV approach is smaller (larger) than that obtained from the DM approach.

In Fig. 3 we have shown the curves of $\tilde{W}$ and $\tilde{W}^{\rm AV}$ as functions of $\Omega_{\rm c}$ [panel (a)] and Δ_3 [panel (b)], respectively.

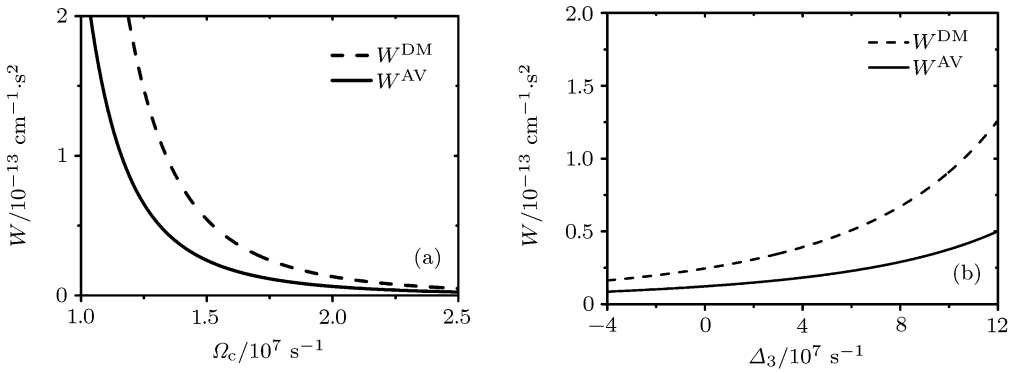


Fig. 3. A comparison between $\tilde{W}$ and $\tilde{W}^{\rm AV}$. (a): The curves of $\tilde{W}$ (dashed line) and $\tilde{W}^{\rm AV}$ (solid line) versus $\Omega_{\rm c}$. (b): The curves of $\tilde{W}$ (dashed line) and $\tilde{W}^{\rm AV}$ (solid line) versus Δ_3.

We see that the SPM effect under the description of DM approach is a little stronger than that under the description of AV approach for different Ω_c and Δ_3, but the difference between them is small.

6. Discussion and conclusion

In order to make further confirmation on the soliton solutions and check their stability, numerical simulations starting directly from the Maxwell–Bloch Eqs. (3) and (4) have been made by taking the soliton solution given by $\Omega_p(0,t)\tau_0 = 8.71\,\mathrm{sech}(1.3t/\tau_0)$ as an initial condition without using any approximation. The waveshape of $|\Omega_p/U_0|^2$ as a function of z is shown in Fig. 4(a).

We see that the probe pulse suffers no serious distortion during the propagation in a long distance for $z = 1.2$ cm. The pulse forms a soliton at about $z = 0.5$ cm. We have also made a simulation directly from the Maxwell–Schrödinger Eq. (5) with the same initial condition without any approximation. The corresponding evolution waveshape is given in Fig. 4(b). We see that there is no apparent difference between the results obtained by the DM and the AV approaches.

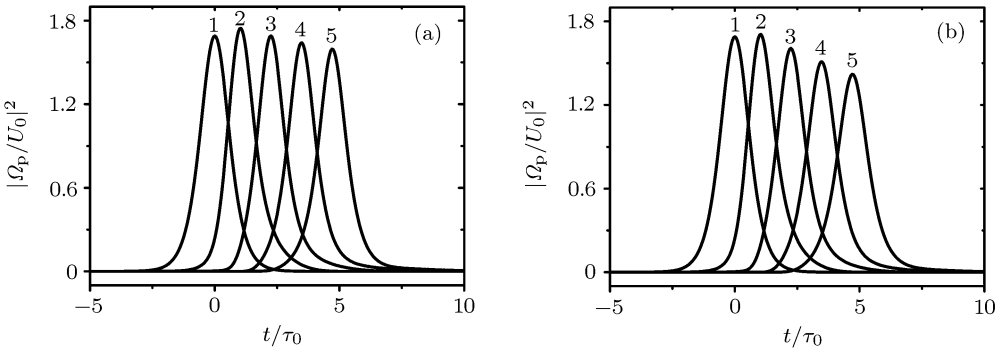


Fig. 4. Evolution plots of the probe pulse in different distances. Panel (a) and panel (b) are respectively for the DM and the AV approaches, with the same initial condition $\Omega_p(0,t)\tau_0 = 8.71\mathrm{sech}(1.3t/\tau_0)$. Lines 1, 2, 3, 4, and 5 are the pulse shapes for $z = 0$, 0.3, 0.6, 0.9, and 1.2 cm, respectively.

The properties of collision between two ultraslow optical solitons are also investigated numerically based on the Maxwell–Bloch Eqs. (3) and (4) by taking $\Omega_p(0,t)\tau_0 = 6.73\,\mathrm{sech}(1.0(t+3.5)/\tau_0) + 8.04\,\mathrm{sech}[1.2t/\tau_0]$ as an initial condition without any approximation. The waveshape of $|\Omega_p/U_0|^2$ is demonstrated in Fig. 5(a). The initial separation of the two solitons is $T_0 = 3.5$ μs and the collision occurs at about $z = 0.5$ cm. one sees that the solitons are robust during the collision. We have also made the simulation on collisions starting from the Maxwell–Schrödinger Eq. (5) with the same initial condition. The corresponding waveshape is shown in Fig. 5(b). Again, we see that there is no apparent difference between the results for the two-soliton collisions in the both DM and AV approaches.

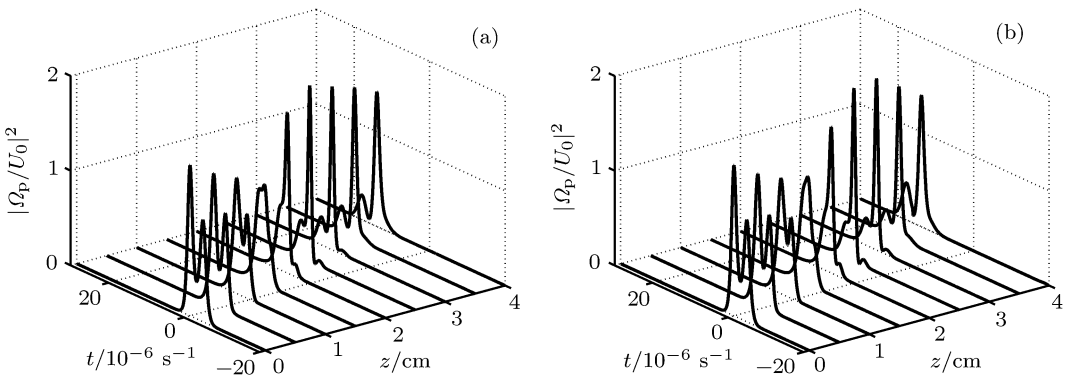


Fig. 5. Evolution plots of the collision between two ultraslow optical solitons. Panel (a) and panel (b) are respectively for DME approach and AV approach, with the same initial condition $\Omega_p(0,t)\tau_0 = 6.73\mathrm{sech}(1.0(t+3.5)/\tau_0) + 8.04\mathrm{sech}[1.2t/\tau_0]$.

In conclusion, we have presented a study of ultraslow optical solitons in a cold, resonant three-level atomic system via EIT under the DM approach. A method of multiple-scales for nonlinear excitations in such resonant system described by the Maxwell–Bloch equations has been developed. The results of the optical properties in both linear and nonlinear regimes have compared carefully with those obtained by using the AV approach. It is found that the results for the both approaches are the same in the linear regime if the corresponding relations between the population-coherence decay rates in the DM approach and the energy-level decay rates in the AV approach are suitably imposed. However, in the nonlinear regime there is a small difference for the SPM coefficient of the NLS equation that governs the time evolution of probe pulse envelope. All analytical predictions in the DM approach and the comparisons between the DM and AV approaches have been checked by numerical simulations.

References

[1] Dauxois T and Peyrard M 2006 *Physics of Solitons* (Cambridge: Cambridge University Press)

[2] Huang G 2005 *Nonlinear Amplitude Equations and Solitons in Bose-Einstein Condensates* In: *Nonlinear Waves in Fluids: Recent Advances and Modern Applications*, CISM Courses and Lecture Notes No. 483 edited by Grimshaw R (Berlin: Springer) pp169–196

[3] Hasegawa A and Matsumoto M 2003 *Optical Solitons in Fibers* (Berlin: Springrer)

[4] Harris S E 1997 *Phys. Today* **50** 36

[5] Fleischhauer M, Imamoglu A and Marangos J P 2005 *Rev. Mod. Phys.* **77** 633 (and references therein)

[6] Hau L V, Harris S E, Dutton Z and Behrrozi C H 1999 *Nature* **397** 594

[7] Kash M M, Sautenkov V A, Zibrov A S, Hollberg L, Welch G R, Lukin M D, Rostovtsev Y, Fry E S and Scully M O 1999 *Phys. Rev. Lett.* **82** 5229

[8] Wu Y and Deng L 2004 *Phys. Rev. Lett.* **93** 143904

[9] Wu Y and Deng L 2004 *Opt. Lett.* **29** 2064

[10] Huang G, Deng L and Payne M G 2005 *Phys. Rev.* E **72** 016617

[11] Huang G, Jiang K, Payne M G and Deng L 2006 *Phys. Rev.* E **73** 056606

[12] Deng L, Payne M G, Huang G and Hagley E W 2005 *Phys. Rev.* E **72** 055601 (R)

[13] Hang C, Huang G and Deng L 2006 *Phys. Rev.* E **73** 036607

[14] Hang C, Huang G and Deng L 2006 *Phys. Rev.* E **74** 046601

[15] Wang J, Hang C and Huang G 2007 *Phys. Lett.* A **366** 528

[16] Hang C and Huang G 2008 *Phys. Rev.* A **77** 033830

[17] Ding J W, She Y C and Wang D L 2009 *Acta Phys. Sin.* **58** 3198 (in Chinese)

[18] Zhuang F, Shen J Q and Ye J 2007 *Acta Phys. Sin.* **56** 541 (in Chinese)

[19] Wang F Y, Shi B S, Lu X S and Guo G C 2008 *Chin. Phys.* B **17** 1798

[20] Li J H, Yang W X and Peng J C 2004 *Chin. Phys.* **13** 1694

[21] Boyd R W 2003 *Nonlinear Optics* (second edition) (San Diego: Academic Press)